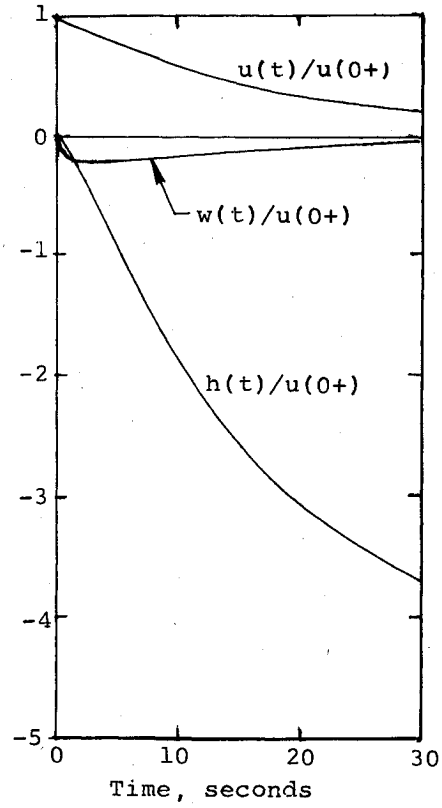

Fig. 1 Velocity and height perturbations, jet transport in landing approach.

The root $s - X_u^*$ is an approximation to the "airspeed" root of Eq. (3). The time constant τ is thus an approximate "airspeed time constant." It is given by

$$\tau = -1/X_u^* \tag{5}$$

where

$$X_u^* = -(\rho S U_0 C_D/m) + (\partial T/\partial u)/m$$

Numerical Values

Airspeed time constants for two quite different commercial aircraft are derived for the full-flap landing approach configuration, at sea level, as appears in Table 1.

The light twin's airspeed time constant is about two-thirds that for the large jet transport. This should be reflected in less sensitivity to wind shear for the smaller aircraft. However, the airspeed time constants for both aircraft are long compared with pilot response time.

The thrust term in X_u^* and τ is only about 10% of the total. Thus, thrust can be neglected to obtain a useful generalized chart that shows the major influences on airspeed time constant, as in Fig. 2. Increased airspeed, lower wing loadings, and higher drag all produce favorable small time constants.

Conclusions

1) Small values of airspeed time constant provide an inherent rapid recovery of airspeed following drop in head wind under wind shear conditions.

2) Small values of airspeed time constant correspond to high airspeed, low wing loading, and high drag coefficient.

3) Landing approach with excess airspeed and in a high drag configuration, such as full flaps and speed brakes partially open, may be beneficial if wind shear is anticipated, to improve airspeed stability.

4) The airspeed time constant for a general aviation light twin aircraft is about two-thirds that of a commercial jet transport.

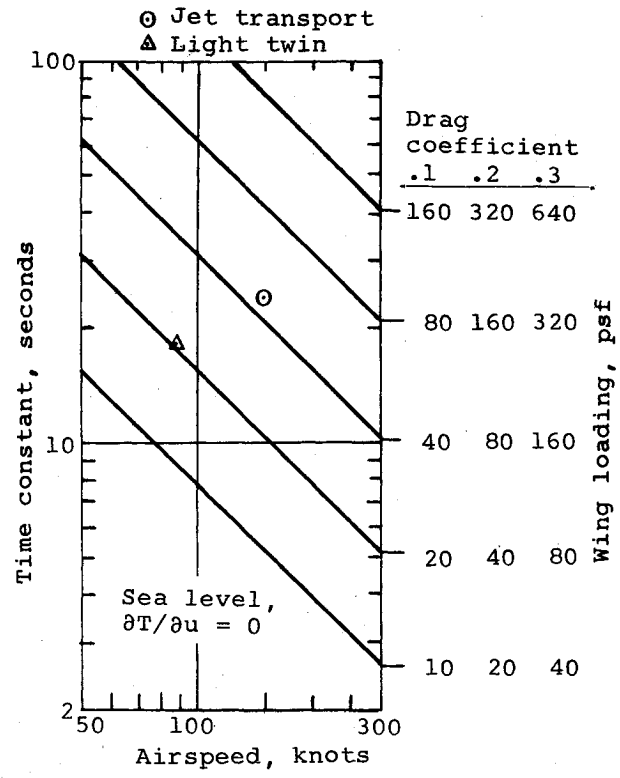

Fig. 2 Variation of airspeed time constant with drag, wing loading, and airspeed.

References

[1] Snyder, C.T., "Analog Study of the Longitudinal Response of a Swept-Wing Transport Airplane to Wind Shear and Sustained Gusts During Landing Approach," NASA TN D-4477, April 1968.

[2] McRuer, D., Ashkenas, I., and Graham, D., *Aircraft Dynamics and Automatic Control*, Princeton Univ. Press, Princeton, N.J., 1973, p. 256.

Small Turbine Guide Vanes Loss Reduction

W. Tabakoff* and W. Hosny†
University of Cincinnati, Cincinnati, Ohio

Introduction

CURRENT applications show the need for advanced small gas turbine engines with high power/weight ratio, low specific fuel consumption, and small size. The helicopter and automotive gas turbine engines are examples of the need for such small engines.

Turbines used in small engines are characterized by their low weight, small size, and highly loaded blades. Losses in these turbines are large and cause a considerable reduction in turbine efficiency. Most of the existent experimental and analytical analyses of turbine losses are for large blade aspect ratio and are, therefore, not applicable to small, highly loaded turbines. The combination of the long chords together with

Presented as Paper 76-617 at the AIAA/SAE 12th Propulsion Conference, Palo Alto, Calif., July 26-29, 1976; submitted Sept. 14, 1976; revision received Oct. 28, 1976.

Index category: Nozzle and Channel Flow.

*Professor, Department of Aerospace Engineering. Associate Fellow AIAA.

†Postdoctoral Fellow, Department of Aerospace Engineering. Member AIAA.

the short blade heights results in small blade aspect ratio in the range of 0.4 to 0.8 which characteristically leads to excessively high secondary flow losses. Meaningful improvements in efficiency must, therefore, be aimed at reducing the secondary flows.

Secondary Flow and Losses

The different flow patterns associated with secondary flows are understood adequately, but the magnitude of the losses is not. Hosny and Tabakoff[1] developed a three-dimensional analysis to predict the rotational flow due to secondary vorticity in highly loaded cascades; the analysis can be used for small aspect ratio blades. Numerous empirical and semiempirical relationships have been used to evaluate the secondary losses in turbomachinery cascades. References 2 and 3 give an extensive review of such relations. The relations usually are limited, however, to the nominal cases associated with each particular relation. In addition, the secondary flow is affected strongly by the upstream boundary-layer thickness. This view is supported by the evidence shown by Turner,[4] who removed the upstream wall boundary layer and found lower losses. The different methods for reduction of secondary losses are given by Tabakoff and Hosny.[5] The most frequently used approaches are: local airfoil recontouring, end wall contouring, flow fences, corner fillets, meridional vane constriction, and vane or blade tilting.

Test Results and Discussion

In the present work, extensive measurements were obtained at the inlet and exit of a vane with 23 nozzles. The purpose of this study is to present the preliminary findings concerning a new technique for controlling the secondary flow losses in a nozzle guide vane. The results of these investigations will be presented only in terms of the total pressure losses for the following three cases: 1) the guide vane with an inlet flow velocity profile that has appreciable end wall boundary layers; 2) the guide vane with an inlet flow velocity profile which has a mid-span wake; and 3) the guide vane with annular splitter ring attached to the nozzle blade leading edge.

The tests were run for a mass flow of 1.09 lb/sec, and the nozzle exit Mach number was about 0.4. The average turning angle of the nozzle airflow was about 70°.

Small calibrated total and directional pressure probes were used upstream and downstream of the guide vane to survey the different flow parameters at the nozzle inlet and exit. A survey of the flow total pressure at exit and inlet was conducted for the three cases. These local total pressure loss distributions were mass averaged over the nozzle pitch, and used in the total pressure loss calculation. The results are presented in terms of the pressure loss coefficient, which is defined as $Y=(P_{t1}-P_{t2})/(P_{t2}-P_2)$ where P_{t1} and P_{t2} are the flow inlet and exit total pressures, respectively, and P_2 is the flow exit static pressure.

The radial distribution of the circumferential average loss coefficient is shown in Fig. 1 for the first two test cases. Comparing the two curves, it can be seen that the losses decreased significantly near the hub when the wake was introduced by the spoiler. This is attributed to the change in the hub boundary layer at the inlet due to the wake. The vane total pressure loss coefficients were calculated by evaluating the area under the two curves of Fig. 1 and the results are: average loss coefficient without inlet wake = 0.1165, average loss coefficient with inlet wake = 0.1065. Thus, the wake creation caused a net reduction in the averaged total losses. In general, the creation of the wake caused a reduction in the secondary losses, while increasing the profile losses in the meantime. The net effect was that of lower overall losses.

With these encouraging results, the experiments were repeated with the annular splitter assembled to the leading portion of the guide vanes. For the purpose of comparison, the spanwise distributions of the pitchwise averaged loss coefficients are shown in Fig. 2 for this case and the first test

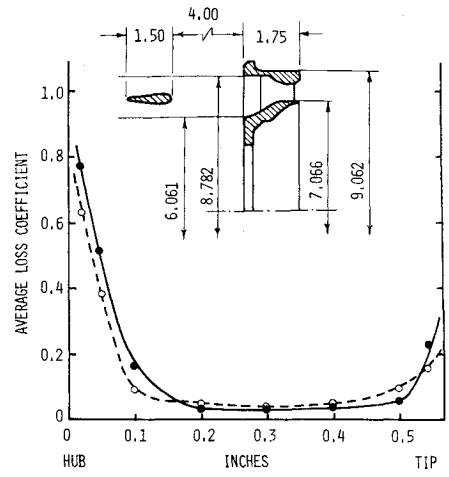

Fig. 1 Average loss radial distribution with and without midspan inlet wake: ● without wake; ○ with wake.

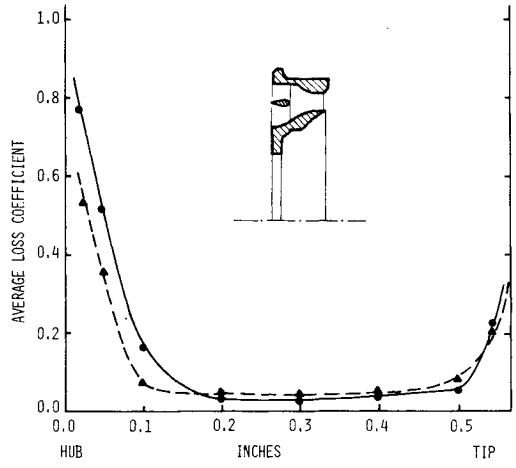

Fig. 2 Average loss distribution in stator nozzle with and without splitter ring: ● without splittering; ▲ with splitter ring.

case. Taking a spanwise average of these distributions, the following total loss coefficients are obtained: loss coefficient without splitter ring = 0.1165, loss coefficient with splitter ring = 0.1006. Thus, again, it can be concluded that the same tendencies prevail as in the case with inlet wake. The splitter increased slightly the profile loss; however, the secondary losses are decreased significantly. The net reduction in the losses was about 14% of the total losses.

Conclusions

The present experimental work shows that additional reduction in the total losses can be achieved by also using an annular splitter at the guide vane entrance region. The annular splitter can be expected to provide a means for controlling the losses in turbine rotors.

Acknowledgment

This research work was sponsored by the U. S. Army Research Office—Durham under Contract Number DAHC04-69-C-0016.

References

[1] Hosny, W. and Tabakoff, W., "An Analysis of the Three Dimensional Flow Problem," AIAA Paper 76-372, July 14-16, 1976, San Diego, Calif.

[2] Hosny, W. and Tabakoff, W., "An Analysis of Losses and Secondary Flow in Turbine Cascades," Project Themis Report 71-23, Dec. 1971 (AD-736853).

[3]Dunham, J., "A Review of Cascade Data on Secondary Lossess in Turbines," *Journal of Mechanical Engineering Science*, Vol. 12, Feb. 1970, pp. 48-59.

[4]Turner, J. R., "An Investigation of the End-Wall Boundary Layer of a Turbine-Nozzle Cascade," *Transactions of American Society of Mechanical Engineering*, Vol. 79, 1957, pp. 1801-1806.

[5]Tabakoff, W. and Hosny, W., "An Experimental Investigation of Loss Reduction in Small Guide Vanes," AIAA Paper 76-617, Palo Alto, Calif., July, 1976.

A Sensitive Torque Meter for Wind-Tunnel Applications

Richard S. Snedeker*
Aeronautical Research Associates of Princeton, Inc., Princeton, N.J.

A REQUIREMENT to measure the rolling moment on a small wing in a wind tunnel has led to the development of a simple yet highly sensitive torque meter. With a span of 6.6 cm (2.6 in.) and a freestream velocity of 14 m/sec (45 ft/sec) the magnitude of the expected rolling moment on this wing was estimated to be a maximum of only 10 gm-cm (0.14 oz-in.). This low torque level and the size of the wind-tunnel test section, 30.5×30.5 cm (1ft×1ft), resulted in the need for a compact instrument that could resolve torques of the order of 1 gm-cm (0.014 oz-in.) or less. Simplicity and economy of construction also were desired. Several concepts were considered, including strain gage load cells, reflected light beams, and servo-driven null systems. However, none was found which met the combined requirements.

A satisfactory device finally was developed which did meet the requirements, and also was insensitive to bending moments and axial and radial loads. The instrument, shown in Fig. 1, incorporates a central element mounted on springs of the flexural pivot type within a fixed tubular case. When torque is applied, a slight rotation is allowed which is sensed by a rotary variable differential transformer (RVDT). In a size suited to this application (0.48-cm, 3/16-in. o.d.) the flexural pivots, manufactured by the Bendix Corporation, are available with torsional spring rates as low as 0.8 gm-cm/deg (0.011 oz-in./deg). Manufacturer's data show that their response to torsion is virtually unaffected by radial and axial loads of the magnitudes anticipated. The RVDT is made by Pickering and Co. (Model No. 21300) and has separate rotor and stator sections. In combination with the flexural pivots, the action of the instrument is frictionless. In principle, the resolution is limited only by the means used to detect the output of the RVDT. As shown in the drawing, the frontal area (3.81-cm, 1.5-in., diam) is limited mainly by the size of the RVDT, which, in this case, is the smallest available of the desired type. The design easily is adapted to RVDT's of smaller diameter should they be available. For extremely small size, the RVDT could be made an integral part of the instrument.

Figure 2 shows how the parts are assembled to allow the desired response. The spiders, which support the forward end of each flexural pivot, are fixed to the outer case by the clamping action of the jam nut against the spacer tubes and the stop ring (also see Fig. 1). The aft ends of the flexural pivots are inserted in holes in the two aft-most pieces of the three-piece rotor, where they are held by set screws. The cutouts in the rotor pieces allow the legs of the spiders to extend to the outer case and provide for the limited rotation of the rotor in response to applied torque. In Fig. 3, the torque meter is shown mounted in a traversing mechanism outside the tunnel.

The amount of rotation is controlled through the choice of the flexural pivot spring rate. For the rolling moment measurements, it was desired to minimize the rotation so that the wing attitude could be considered fixed. At the same time the motion had to be sufficient to produce a measurable response by the RVDT. Some typical data will illustrate the characteristics of the instrument.

The flexural pivots each had a torsional spring rate of 6.56 gm-cm/deg (0.091 oz-in./deg) (Bendix Cat. No. 5006-600). Thus, the two in combination gave an instrument spring rate of 13.1 gm-cm/deg (0.18 oz-in./deg) or a rotary sensitivity of 0.076 deg/gm-cm (5.5 deg/oz-in.). The RVDT was excited by a 10 kHz signal of 3 Vrms amplitude, and the output was demodulated through a diode circuit having a zero adjustment

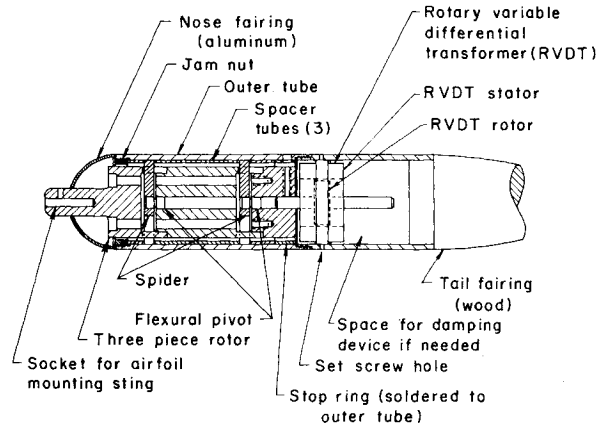

Fig. 1 Longitudinal cross section of torque meter. All parts are stainless steel unless noted.

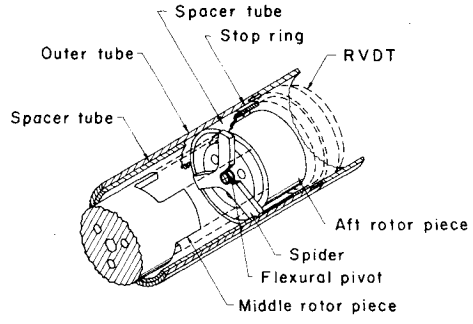

Fig. 2 Cut-away view showing assembly of flexural pivot and related parts.

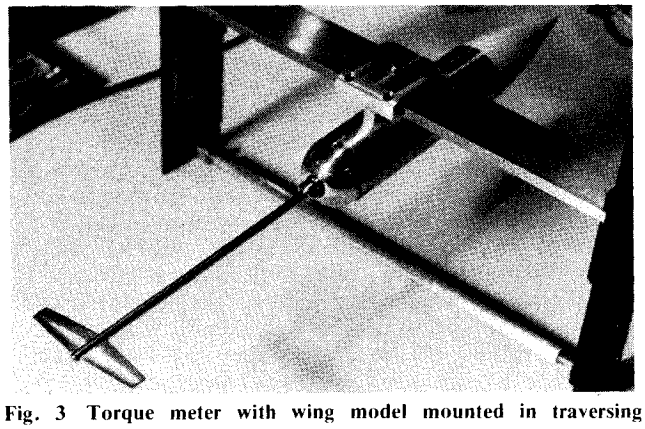

Fig. 3 Torque meter with wing model mounted in traversing mechanism.

Received Sept. 30, 1976.
Index category: Research Facilities and Instrumentation.
*Consultant. Member AIAA.